Heavy fermion spin liquid in herbertsmithite

V. R. Shaginyan,[1,2,*] M. Ya. Amusia,[3,4] A. Z. Msezane,[2] K. G. Popov,[5] and V. A. Stephanovich[6]

[1]*Petersburg Nuclear Physics Institute, NRC Kurchatov Institute, Gatchina, 188300, Russia*
[2]*Clark Atlanta University, Atlanta, GA 30314, USA*
[3]*Racah Institute of Physics, The Hebrew University, 91904 Jerusalem, Israel*
[4]*Ioffe Physico-Technical Institute,194021 St. Petersburg, Russia*
[5]*Komi Science Center, Ural Division, RAS, Syktyvkar, 167982, Russia*
[6]*Institute of Physics, Opole University, Opole Poland*

We analyze recent heat capacity measurements in herbertsmithite $ZnCu_3(OH)_6Cl_2$ single crystal samples subjected to strong magnetic fields. We show that the temperature dependence of specific heat C_{mag} formed by quantum spin liquid at different magnetic fields B resembles the electronic heat capacity C_{el} of the HF metal $YbRh_2Si_2$. We demonstrate that the spinon effective mass $M^*_{mag} \propto C_{mag}/T$ exhibits a scaling behavior like that of C_{el}/T. We also show that the recent measurements of C_{mag} are compatible with those obtained on powder samples. These observations allow us to conclude that $ZnCu_3(OH)_6Cl_2$ holds a stable strongly correlated quantum spin liquid, and a possible gap in the spectra of spinon excitations is absent even under the application of very high magnetic fields of 18 T.

PACS numbers: 75.40.Gb, 71.27.+a, 71.10.Hf

Quantum spin liquids (QSLs) are promising new phases, where exotic quantum states of matter could be realized. Although much theoretical effort has been devoted to understand their physical nature, the question is still far from its complete clarification. Generally speaking, the QSL is a quantum state, formed with hypothetic particles like fermionic spinons carrying spin 1/2 and no charge. A number of QSLs with various types of ground states are proposed [1–18] but the lack of real materials possessing them obscure the underlying physical mechanism. On the other hand, one needs a real theory that plays important role in the understanding and interpreting accessible experimental facts [19–22]. Measurements on magnetic insulators with geometrical frustration produce important experimental data shedding light on the nature of spinon composing QSL. Recent measurements indicate that the insulator $ZnCu_3(OH)_6Cl_2$ (herbertsmithite) is very likely to be the first promising candidate to host a QSL in real bulk materials. In herbertsmithite, the dynamic magnetic susceptibility shows that at low temperatures quasiparticle excitations, or spinons, form a continuum, and populate an approximately flat band crossing the Fermi level [17, 21]. At the same time, our analysis of herbertsmithite thermodynamic properties allows us to reveal their scaling behavior. The above results demonstrate that the properties of the herbertsmithite are similar to those of heavy-fermion (HF) metals. Thus, it can be viewed as a new type of strongly correlated HF electrical insulator exhibiting properties of HF metals but resisting electric current [20–22].

The development of this concept, however, faces fundamental problems still remaining to be resolved. The first one is that the experimental data are taken in measurements on herbertsmithite powder samples [4–6, 20–22]. As a result, both out-of-plane magnetic defects and site disorder between the Cu and Zn ions can strongly change the behavior of the bulk susceptibility or even alter its low-temperature scaling at weak magnetic fields, see e.g. Ref. [16]. The second problem is based on experimental data showing that QSL in the herbertsmithite is unstable against the application of external magnetic fields. This instability is represented by the emergence of so-called spin-solid phase, which, in turn, is separated from the spin-liquid one by a gap induced by an applied magnetic field [23]. Thus, the experimental observations of QSL remain scattered and need regimentation. In our opinion, this can be partially achieved by presenting a reliable interpretation of the recent measurements of specific heat C in high magnetic fields performed on herbertsmithite single crystal samples [24, 25].

In this Communication we analyze the recent heat capacity C measurements in strong magnetic fields on herbertsmithite. We interpret the above measurements in terms of QSL spinon contribution. To obtain the spinon - determined partial specific heat C_{mag}, we subtract the phonon and Schottky effect contributions from the total heat capacity C. It turns out that obtained C_{mag} as a function of temperature T at fixed magnetic field B behaves very similarly to the electronic specific heat C_{el} of the HF metal $YbRh_2Si_2$. This observation allows us to conclude that spinons form the Fermi sphere with the Fermi momentum p_F, while the gap in the spectra of spinon excitations and the spin-solid phase are absent. We demonstrate that the effective mass of spinon $M^*_{mag} \propto C_{mag}/T$ exhibits a scaling behavior resembling that of C_{el}/T. We also show that new measurements of C_{mag} on single crystal samples are compatible with those obtained on powder samples.

The $S = 1/2$ spins of the Cu^{+2} ions occupy the positions in a highly symmetric kagome lattice. As spins on

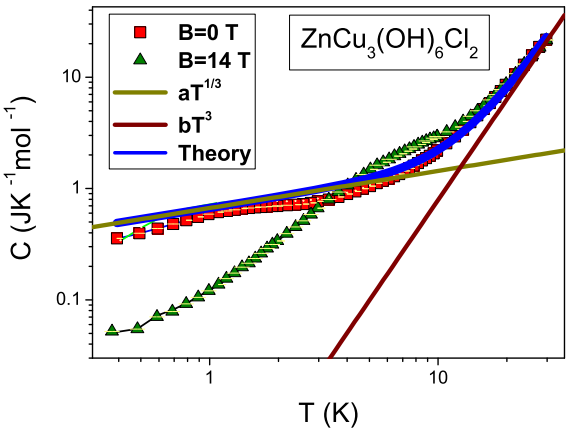

FIG. 1: (color online). The heat capacity measurements on single crystal of $ZnCu_3(OH)_6Cl_2$ at $B = 0$ (squares) and $B = 14$ T (triangles) [24, 25]. The thick blue line corresponds to our theoretical approximation (5) with fitting parameters a and b. The lines represent $C = aT^{1/3}$ and $C = bT^3$, see legend.

the above lattice reside in a highly symmetric structure of corner-sharing triangles, the ground state energy does not depend on the spins configuration. As a result, spins located at the kagome hexagon, composed of the two triangles, form a (frustrated) pattern that is even more frustrated than the triangular lattice considered by Anderson [26]. As a result, the kagome lattice has a flat topologically protected branch of the spectrum with zero excitation energy [27, 28]. Therefore, the fermion condensation quantum phase transition (FCQPT) can be considered as a quantum critical point (QCP) of the $ZnCu_3(OH)_6Cl_2$ QSL [20, 30]. In that case, we expect that at low temperatures the heat capacity C of herbertsmithite becomes a function of the applied magnetic field, as it is seen from Fig. 1. We propose that mentioned QSL is composed of chargeless fermions called spinons with the effective mass M^*_{mag}. Latter fermions with spin $\sigma = 1/2$ occupy the corresponding Fermi sphere with the Fermi momentum p_F, and form the excitation spectrum typical for HF liquid located near FCQPT, while spinons represent HF quasiparticles of deconfined QSL. Thus, the ground state energy $E(n)$ is given by the Landau functional depending on the spinon distribution function $n_\sigma(\mathbf{p})$, where $\mathbf{p}$ is the momentum. Near FCQPT point, the effective mass M^*_{mag} is governed by the Landau equation [29–31]

$$\frac{1}{M^*_{mag}(T,B)} = \frac{1}{M^*_{mag}(T=0,B=0)} + \frac{1}{p_F^2}\sum_{\sigma_1}\int \frac{\mathbf{p}_F\mathbf{p}_1}{p_F} F_{\sigma,\sigma_1}(\mathbf{p_F},\mathbf{p}_1)\frac{\partial\delta n_{\sigma_1}(\mathbf{p}_1)}{\partial p_1}\frac{d\mathbf{p}_1}{(2\pi)^3}. \quad (1)$$

Here we have rewritten the spinon distribution function as $\delta n_\sigma(\mathbf{p}) \equiv n_\sigma(\mathbf{p},T,B) - n_\sigma(\mathbf{p},T=0,B=0)$. The Landau interaction F is defined by the fact that the system has to be at FCQPT. Thus, this interaction brings the system to FCQPT point, where Fermi surface alters its topology so that the effective mass acquires temperature and field dependence [30, 32, 33]. At this point, the term $1/M^*_{mag}(T=0,B=0)$ vanishes and Eq. (1) becomes homogeneous. It can then be solved analytically. At $B = 0$, the effective mass depends on T demonstrating the NFL (non-Fermi liquid) behavior

$$M^*_{mag}(T) \simeq a_T T^{-2/3}. \quad (2)$$

At finite T, the application of magnetic field B drives the system to Landau Fermi liquid (LFL) region with

$$M^*_{mag}(B) \simeq a_B B^{-2/3}. \quad (3)$$

At finite B and T near FCQPT, the solutions of Eq. (1) $M^*_{mag}(B,T)$ can be well approximated by a simple universal interpolating function. The interpolation occurs between the LFL ($M^*(T) \propto const$) and NFL ($M^*_{mag}(T) \propto T^{-2/3}$) regions. As it is seen from Eq. (3), under the application of magnetic field M^*_{mag} becomes finite, and at low temperatures the system demonstrates the LFL behavior $C_{mag}(T)/T \propto M^*_{mag}(T) \simeq M^*_{mag}(T=0) + a_1T^2$. Then, as it is seen from Fig. 2, at increasing temperatures $M^*_{mag} \propto C_{mag}/T$ grows, and enters a transition regime, reaching its maximum $M^*_{\max} \propto (C_{mag}(T)/T)_{\max}$ at $T = T_{\max}$, with subsequent diminishing given by Eq. (2).

To reveal a scaling behavior, we introduce the normalized effective mass M^*_N and the normalized temperature T_N dividing the effective mass M^*_{mag} by its maximal values, $M^*_{\max}$, and temperature T by $T_{\max}$ at which the maximum occurs. The normalized effective mass $M^*_N = M^*/M^*_{\max}$ as a function of the normalized temperature $y = T_N = T/T_{\max}$ is given by the interpolating function that approximates the solution of Eq. (1) [30, 31]

$$M^*_N(y) \approx c_0\frac{1+c_1y^2}{1+c_2y^{8/3}}. \quad (4)$$

Here $c_0 = (1+c_2)/(1+c_1)$, c_1 and c_2 are fitting parameters, c_1 and c_2 are fitting parameters, parameterizing the Landau interaction. Magnetic field B enters Eq. (1) only in the combination μ_BB/k_BT, making $k_BT_{\max} \simeq \mu_BB$ where k_B is Boltzmann constant and μ_B is Bohr magneton [30, 32]. Thus, Eq. (4) exhibits the scaling behavior, which is the intrinsic property of Eq. (1) at FCQPT: M^*_N at different magnetic fields merges into a single curve as a function of the variable y. In what follows we use Eq. (4) to clarify our calculations based on Eq. (1).

To analyze the spinon specific heat $C_{mag}(T,B)$, we have to exclude the contribution coming form lattice (phonons) that is independent of B. To separate C_{mag} contribution, we approximate $C(T,B=0)$ by the function

$$C(T) = aT^{1/3} + bT^3. \quad (5)$$

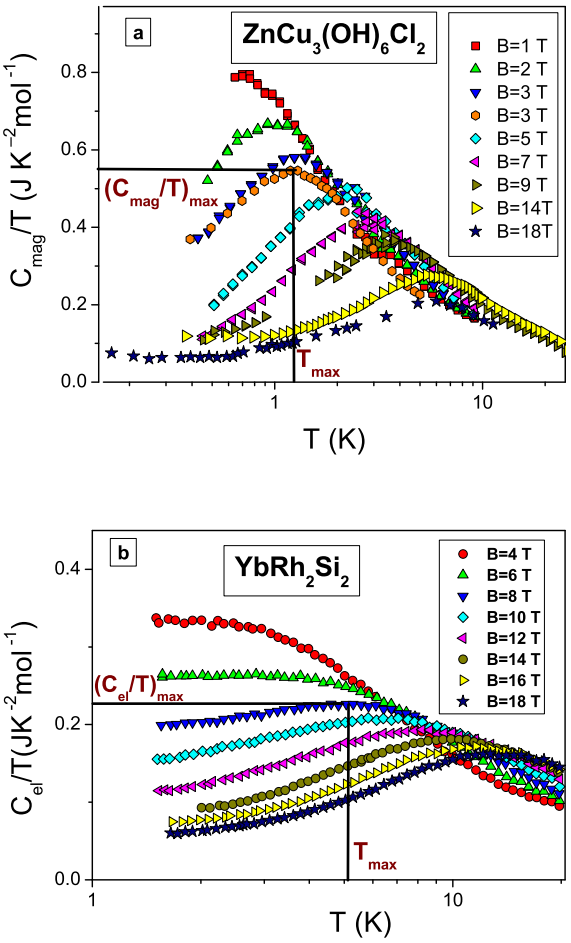

FIG. 2: (color online). Panel a: The specific heat C_{mag}/T of $ZnCu_3(OH)_6Cl_2$ measured on powder [5] and single crystal samples [24, 25]. (C_{mag}/T) is displayed as a function of temperature T for fields B shown in the legends. Panel b: The specific heat C_{el}/T extracted from measurements on the HF metal $YbRh_2Si_2$ [34] exhibits the same behavior as C_{mag}/T. The illustrative values of the maxima $(C_{mag}/T)_{\max}$ and $(C_{el}/T)_{\max}$ of both C_{mag}/T and C_{el}/T and the corresponding $T_{\max}$ are also shown in panels a and b.

Here the first term proportional to $M^*_{mag}(T) \propto T^{1/3}$ presents the QSL contribution when it exhibits the NFL behavior, as it follows from Eq. (2), while the second one is determined by the lattice (phonon) contribution. It is seen from Fig. 1, that the approximation (5) is valid in a wide temperature range. At low temperatures $T \leq 4$ K the heat capacity is mainly formed by spinons, while the phonon contribution prevails at higher temperatures, making its main contribution at $T \geq 10$ K. It is seen, that at diminishing temperatures the LFL behavior, $C \propto T$, starts to form. We note, that the Schottky anomaly was removed, as it is usually done, see e.g. [24, 25]. Upon comparing the data on the heat capacity taken at $B = 9$ and $B = 14$ T shown in Fig. 1,

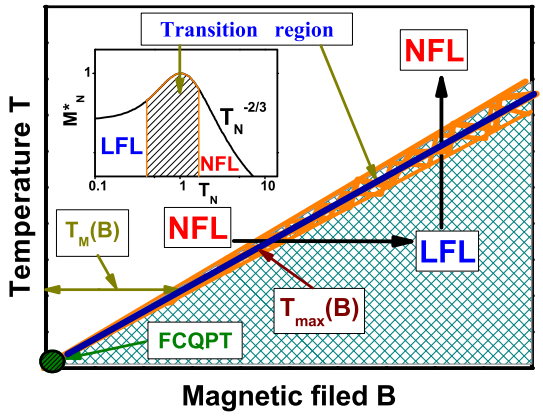

FIG. 3: (color online). Schematic $T-B$ phase diagram of SCQSL with magnetic field as control parameter. The vertical and horizontal arrows show LFL-NFL and reverse transitions at fixed B and T, respectively. The hatched areas in the inset and main panel shown by the arrows represent the transition region at $T_{\max}(B)$. The solid line in the hatched area represents the function $T_{\max}(B) \sim T_M(B)$. The functions $T_M(B)$ shown by two-headed arrows define the total widths of the NFL state and the transition area. The inset shows a plot of the normalized effective mass M^*_N versus the normalized temperature T_N. Transition region, where M^* reaches its maximum $M^*_{\max}$ at $T_N = T/T_{\max} = 1$, is shown by the arrow.

one concludes that C strongly depends on the magnetic field. However, at raising temperatures $T \geq 10$ K the B-dependence vanishes, for the contribution coming from phonons prevails, then, the system enters the transition regime at $k_BT \simeq \mu_BB$, and the influence of magnetic field becomes weak, as shown in the $T-B$ phase diagram, Fig. 3.

The obtained heat capacity of QSL, $C_{mag}/T = (C - bT^3)/T$, is displayed in Fig. 2, panel a. It follows from panel a, that the results obtained on different kinds (powder and single crystal) of samples and in different measurements [4, 5, 24, 25] exhibit similar properties. To show that the behavior of C_{mag}/T reported in panel a is of generic character, we note that $C_{mag}/T \propto M^*_{mag}$ behaves like C_{el}/T shown in panel b. Indeed, as seen from Fig. 2, the maximum structure in C_{mag}/T and C_{el}/T at temperature $T_{\max}$ appears under the application of magnetic field B and $T_{\max}$ shifts to higher T as B is increased. The value of the maximum structure is saturated towards lower temperatures decreasing at elevated magnetic fields. It is worthy to note, that $C_{mag}/T \sim C_{el}/T$, as it is seen from the panels a and b. Thus, QSL of $ZnCu_3(OH)_6Cl_2$ can be viewed as a strongly correlated quantum spin liquid (SCQSL) that behaves like that of the HF metal $YbRh_2Si_2$, exhibiting a gapless behavior in high magnetic fields up to 18 T.

We now construct the schematic phase diagram of $ZnCu_3(OH)_6Cl_2$, reported in Fig. 3. At $T = 0$ and

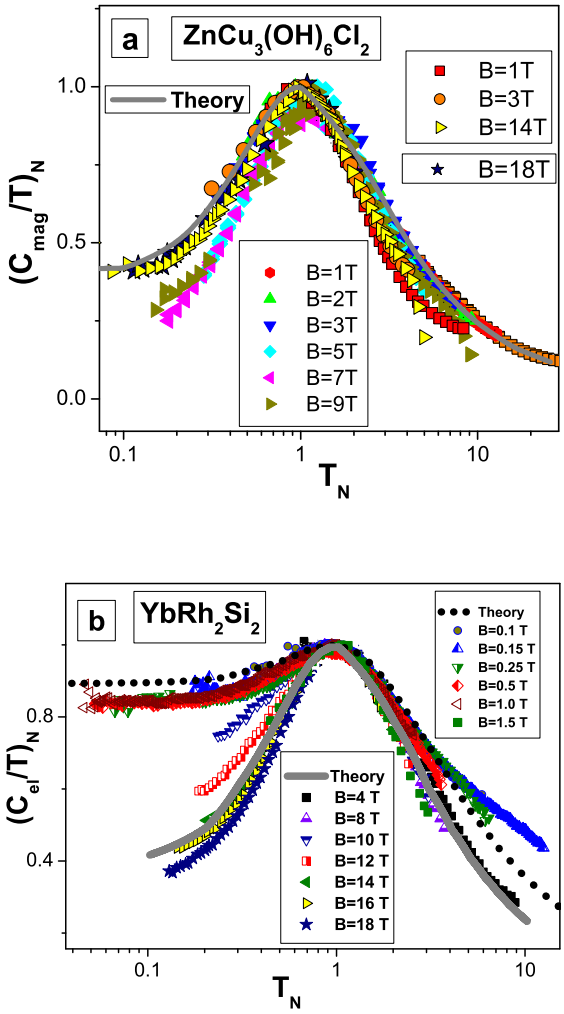

FIG. 4: (color online). Panel a: The normalized specific heat $(C_{mag}/T)_N = M_N^*$ of $ZnCu_3(OH)_6Cl_2$ versus normalized temperature T_N as a function of B shown in the legends. $(C_{mag}/T)_N$ is extracted from the data [5, 24, 25] shown in Fig. 2, panel a. Solid curve represents our calculations, and traces the scaling behavior of the effective mass. Panel b: The normalized specific heat $(C_{el}/T)_N = M_N^*$ of $YbRh_2Si_2$ versus normalized temperature T_N as a function of B at low (upper box symbols) and high (lower box symbols, corresponding to those shown in Fig. 2, panel b) magnetic fields, extracted from the specific heat measurements on the $YbRh_2Si_2$ [34, 35]. The low-field calculations are depicted by the dotted line tracing the scaling behavior of M_N^*. The high-field calculations (solid line) are performed for magnetic fields when the quasiparticle band becomes fully polarized [36].

$B = 0$ the system is approximately located at QCP of FCQPT without tuning. Both magnetic field B and temperature T play the role of the control parameters, shifting the system from its QCP and driving it from the NFL to LFL regions as shown by the vertical and horizontal arrows. At fixed temperatures the increase of B leads the system along the horizontal arrow from NFL to LFL region. This behavior is seen from Fig. 2, panels a and b:

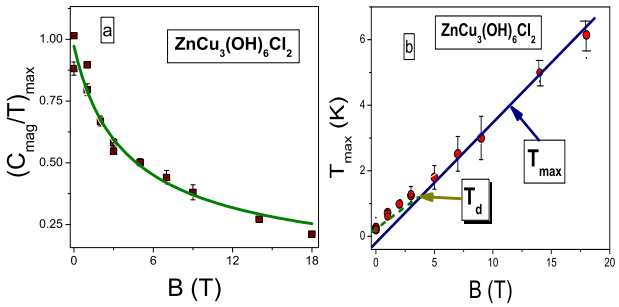

FIG. 5: (color online). Panel a: The maxima $(C_{mag}/T)_{\max}$ of C_{mag}/T versus magnetic field B are shown by the solid squares, see Fig. 2, panel a. The solid curve is approximated by $M^*_{\max}(B) = dB^{-2/3}$, see Eq. (3), where d_1 is a fitting parameter. Panel b: The temperatures $T_{\max}(B)$, at which the maxima of (C_{mag}/T) are located, see Fig. 2, panel a. The solid straight line represents the function $T_{\max} = d_2 B$, d_2 being a parameter. T_d shown by the arrow is the temperature at which the straight line $T^*_{\max}$ starts to deviate from the experimental data, as shown by the dashed line.

The application of B shifts $T_{\max}$ to higher temperatures. On the contrary, at fixed magnetic field and increasing temperatures the system moves along the vertical arrow from the LFL to NFL region. The inset to Fig. 3 demonstrates the behavior of the normalized effective mass M_N^* versus the normalized temperature T_N that follows from Eq. (4). It is seen that the temperature range $T_N \sim 1$ represents the transition region between the LFL regime with almost constant effective mass and the NFL behavior, having the $T^{-2/3}$ dependence. It follows from Eq. (4) and Fig. 3 that the width of the transition region is given by $T_M \propto T_{\max}(B) \propto T \propto B$. The phase diagram in Fig. 3 demonstrates that the properties of $ZnCu_3(OH)_6Cl_2$ are close to those of the HF metal $YbRh_2Si_2$ [30, 31].

Figure 4, panel a, reports the normalized specific heat $(C_{mag}/T)_N = M_N^*$ versus normalized temperature T_N as a function of B. It is seen that at low $T_N \lesssim 0.1$, $(C_{mag}/T)_N \simeq 0.4$. This value is determined by the QSL polarization in magnetic fields, and coincides with that of $(C_{el}/T)_N = M_N^*$ obtained on $YbRh_2Si_2$. In both panels a and b, our calculations are shown by the same solid curve. Note that at low temperatures and magnetic fields, when the polarization is negligible, $(C_{el}/T)_N \simeq 0.9$, as it is seen from panel b of Fig. 4.

In Fig. 5, panel a, the solid squares denote the values of the maxima $(C_{mag}/T)_{\max}(B)$, taken from Fig. 2, panel a. In panel b, the corresponding values of $T_{\max}(B)$ are displayed versus magnetic field B. It is seen that the agreement between the theory and experiment is good. In panel b, the solid straight line represents the function $T_{\max}(B) \propto d_2 B$. It is seen that at relatively high temperatures the experimental data are well approximated by the straight line, while at $T \leq T_d$ there is deviation.

This fact evidences that SCQSL of herbertsmithite is not exactly placed at FCQPT, for in that case the approximation $T_{\max} \propto d_2 B$ would be good at low temperatures. This conclusion coincides with general properties of the phase diagrams of HF metals [37] and with experimental data, showing that at low temperatures C demonstrates the LFL behavior [5, 24, 25], see Fig. 1 as well.

In summary, based on the recent experimental facts, we have shown that $ZnCu_3(OH)_6Cl_2$ can be viewed as a strongly correlated Fermi system whose thermodynamics is defined by SCQSL located at FCQPT. Our calculations of the heat capacity C_{mag}/T are in good agreement with the experimental data and the scaling behavior of C_{mag}/T coincides with that observed in the HF metal $YbRh_2Si_2$ up to high magnetic fields of 18 T. Thus, spinons forming SCQSL remain itinerant even in high magnetic fields. We also have shown that recent measurements of C_{mag} on single crystal samples are consistent with those obtained on powder samples.

We thank T. H. Han for valuable discussions. V.R.S. is supported by the Russian Science Foundation, Grant No. 14-22-00281. A.Z.M. thanks the US DOE, Division of Chemical Sciences, Office of Energy Research, and ARO for research support. P.K.G. is partly supported by RFBR # 14-02-00044 and by SPbSU # 11.38.658.2013.

* Electronic address: vrshag@thd.pnpi.spb.ru

[1] P. W. Anderson, Mater. Res. Bull. **8**, 153 (1973).
[2] F. Mila, Phys. Rev. Lett. **81**, 2356 (1998).
[3] M. P. Shores, E. A. Nytko, B. M. Bartlett, and D. G. Nocera, J. Am. Chem. Soc. **127**, 13462 (2005).
[4] J. S. Helton, K. Matan, M. P. Shores, E. A. Nytko, B. M. Bartlett, Y. Yoshida, Y. Takano, A. Suslov, Y. Qiu, J. H. Chung, D. G. Nocera, and Y. S. Lee, Phys. Rev. Lett. **98**, 107204 (2007).
[5] M. A. deVries, K. V. Kamenev, W. A. Kockelmann, J. Sanchez-Benitez, and A. Harrison Phys. Rev. Lett. **100**, 157205 (2008).
[6] J. S. Helton, K. Matan, M. P. Shores, E. A. Nytko, B. M. Bartlett, Y. Qiu, D. G. Nocera, and Y. S. Lee, Phys. Rev. Lett. **104**, 147201 (2010).
[7] A. Zorko, S. Nellutla, J. van Tol, L. C. Brunel, F. Bert, F. Duc, J. C. Trombe, M. A. deVries, A. Harrison, P. Mendels, Phys. Rev. Lett. 101 (2008) 026405.
[8] S. S. Lee and P. A. Lee, Phys. Rev. Lett. **95**, 036403 (2005).
[9] O. I. Motrunich, Phys. Rev. B **72**, 045105 (2005).
[10] Y. Ran, M. Hermele, P. A. Lee, and X. G. Wen, Phys. Rev. Lett. **98**, 117205 (2007).
[11] S. Ryu, O. I. Motrunich, J. Alicea, and M. P. A. Fisher, Phys. Rev. B **75**, 184406 (2007).
[12] L. Balents, Nature **464**, 199 (2010).
[13] F. Bert and P. Mendels, J. Phys. Soc. Jpn. **79**, 011001 (2010).
[14] S. Yan, D. A. Huse, and S. R. White, Science **332**, 1173 (2011).
[15] T. H. Han, J. S. Helton, S. Chu, A. Prodi, D. K. Singh, C. Mazzoli, P. Müller, D. G. Nocera, and Y. S. Lee, Phys. Rev. B **83**, 100402(R), (2011).
[16] P. Mendels and F. Bert, J. Phys.: Conference Series **320**, 012004 (2011).
[17] T.H. Han, J. S. Helton, S. Chu, D. G. Nocera, J. A. Rodriguez-Rivera, C. Broholm, and Y. S. Lee, Nature **492**, 406 (2012).
[18] M. Punk, D. Chowdhury, and S. Sachdev, Nature Physics **10**, 289 (2014).
[19] V. R. Shaginyan, M. Ya. Amusia, J. W. Clark, G. S. Japaridze, A. Z. Msezane, K. G. Popov, V. A. Stephanovich, M. V. Zverev, and V. A. Khodel, arXiv:1409.4034.
[20] V. R. Shaginyan, A. Z. Msezane, and K. G. Popov, Phys. Rev. B **84**, 060401(R) (2011).
[21] V. R. Shaginyan, A. Z. Msezane, K. G. Popov, and V. A. Khodel, Phys. Lett. A **376**, 2622 (2012).
[22] V. R. Shaginyan, A. Z. Msezane, K. G. Popov, G. S. Japaridze, V. A. Stephanovich, Europhys. Lett. **97**, 56001 (2012).
[23] M. Jeong, F. Bert, P. Mendels, F. Duc, J. C. Trombe, M. A. de Vries, and A. Harrison, Phys. Rev. Lett. **107**, 237201 (2011).
[24] T. H. Han, S. Chu, and Y. S. Lee, Phys. Rev. Lett. **108**, 157202 (2012).
[25] T. H. Han, R. Chisnell, C. J. Bonnoit, D. E. Freedman, V. S. Zapf, N. Harrison, D. G. Nocera, Y. Takano, and Y. S. Lee, arXiv:1402.2693 (2014).
[26] P. A. Lee, Science **321**, 1306 (2008).
[27] D. Green, L. Santos, and C. Chamon, Phys. Rev. B **82**, 075104 (2010)
[28] T. T. Heikkilá, N. B. Kopnin, and G. E. Volovik, JETP Lett. **94**, 252 (2011).
[29] L. D. Landau, Sov. Phys. JETP **3**, 920 (1956).
[30] V. R. Shaginyan, M. Ya. Amusia, A. Z. Msezane, and K. G. Popov, Phys. Rep. **492**, 31 (2010).
[31] M. Ya. Amusia, K. G. Popov, V. R. Shaginyan, V. A. Stephanovich, *Theory of Heavy-Fermion Compounds*, Springer Series in Solid-State Sciences **182**, (2014).
[32] J. W. Clark, V. A. Khodel, and M. V. Zverev, Phys. Rev. B **71**, 012401 (2005).
[33] V. A. Khodel, J. W. Clark, and M. V. Zverev, Phys. Rev. B **78**, 075120 (2008).
[34] P. Gegenwart, Y. Tokiwa, T. Westerkamp, F. Weickert, J. Custers, J. Ferstl, C. Krellner, C. Geibel, P. Kerschl, K. H. Müller, and F. Steglich, New J. Phys. **8**, 171 (2006).
[35] N. Oeschler, S. Hartmann, A. Pikul, C. Krellner, C. Geibel, and F. Steglich, Physica B **403**, 1254 (2008).
[36] V. R. Shaginyan, K. G. Popov, V. A. Stephanovich, V. I. Fomichev, and E. V. Kirichenko, Europhys. Lett. **93**, 17008 (2011).
[37] V. R. Shaginyan, A. Z. Msezane, K. G. Popov, G. S. Japaridze, and V. A. Khodel, Europhys. Lett. **106**, 37001 (2014).